Analysis of Cross-Talk Induced Measurement Errors in Model-Based RF Voltage Sensing

Mathias Poik, Thomas Hackl, Stefano Di Martino, Martin Schober, Jin Dang and Georg Schitter *Senior Member, IEEE*

***Abstract*—Contactless sensing methods using capacitively coupled probes can enable local radio frequency (RF) voltage measurements without the need for large contact pads. This enables a measurement of internal voltage distributions and can significantly facilitate the development of integrated microwave devices. The achievable spatial resolution of these methods is typically limited by parasitic capacitive cross-talk between the probe and adjacent circuit parts. When RF voltage measurements are performed at multiple tip-surface distances, cross-talk can be reduced by employing a suitable model of the distance dependent tip-circuit capacitance. In this paper, the achievable spatial resolution and its limitation by cross-talk induced errors is analysed. Electrostatic simulations of the capacitance between a probe tip and different test structures on a passivated circuit are performed and the results are verified by RF voltage measurements on µm-sized test structures at a frequency of 13 GHz. The analysis shows, that the achievable spatial resolution is mainly limited by the passivation layer and that cross-talk induced measurement errors limit the minimum structure size to two times the layer thickness.**

***Index Terms*—Contactless, capacitive cross-talk, radio frequency (RF), voltage measurement, passive voltage probe**

I. Introduction

The precise knowledge of local radio frequency (RF) voltages is crucial for the design of miniaturized microwave devices. For instance, large active area devices such as antenna switches [1] or power amplifiers [2] often consist of multiple transistors connected in series or parallel. They can have distinct parasitic coupling capacitances to the substrate or in between individual transistors, leading to unwanted distortions of the local voltage distribution within the device. Due to the small size of individual transistors down to a few μm [3] contact-based probing methods are not always applicable for a measurement of the local RF voltages due to the relatively large required contact pad sizes. Although contact-based methods have been used to deduce the voltage distributions from external, input-output based measurements [4], this approach is ultimately limited by the accuracy of the used device model. A direct measurement of local RF voltages with μm spatial resolution would therefore be beneficial for the design of miniaturized microwave devices.

Passive voltage probes have been widely used for contactless measurements on RF circuits [5], [6]. The probes typically consist of a coaxial transmission line with a miniaturized protruding tip, which is brought in close proximity to the surface. The tip capacitively couples to a test point on the circuit to determine the local RF voltage, without the need for electrical contact with the circuit. This enables a direct measurement of RF voltages within devices, in situations where the placement of contact pads is difficult or impossible due to their relatively large size. For instance, passive voltage probes have been applied for measurements on bondwires [7] and between individual transistors (70 μm separation) of power amplifiers [8]. The achievable spatial resolution of this approach is mainly limited by the size of the tip and by cross-talk due to parasitic coupling to adjacent parts of the circuit [9]. In order to maximize the spatial resolution miniaturized tips have been developed [10]. For a further improvement of the spatial resolution typically measurements at two different tip-surface distances are performed and the difference between the measurements is computed [11]. Since the gradient of the local tip-circuit capacitance is highest for test points closest to the tip, the selection of a small distance between the two measurements enables a compensation of cross-talk to adjacent circuit parts with a larger distance to the tip. However, the differential procedure leads to a reduction of the measured signal and the distance therefore has to be selected in a trade-off between spatial resolution and sensitivity.

If measurements at multiple tip-surface distances are available, the trade-off between spatial resolution and sensitivity can be overcome by a model-based approach [12]. By performing continuous RF voltage vs. distance measurements at precisely known tip-surface distances, the capacitive coupling to a local test point can be identified and separated from unwanted cross-talk contributions. The feasibility of the method was verified by RF voltage measurements on interdigital test structures with 2 μm size. However, a detailed analysis of the achievable spatial resolution and its limitations has not been carried out yet.

The contribution of this paper is an analysis of the achievable spatial resolution of model-based RF voltage sensing. To this end, the coupling capacitances between the probe tip and circuit test structures of different dimensions are analysed by electrostatic simulations. The applicability of the model-based measurement method depending on the test structure dimensions is evaluated and the simulation results are verified by RF voltage measurements.

The paper is organized as follows. In Section II the RF voltage sensing system is presented. In Section III, the model-based measurements procedure [12] and its limitations are

M. Poik, T. Hackl, M. Schober and G. Schitter are with the Automation and Control Institute (ACIN), TU Wien, Gusshausstrasse 27-29, 1040 Vienna, Austria (email: poik@acin.tuwien.ac.at).
S. Di Martino and J. Dang are with Infineon Technologies AG, 8020 Graz, Austria.

Pre-print version of the article: Mathias Poik, Thomas Hackl, Stefano Di Martino, Martin Schober, Jin Dang and Georg Schitter, "Analysis of Cross-Talk Induced Measurement Errors in Model-Based RF Voltage Sensing ", *2023 IEEE International Instrumentation and Measurement Technology Conference (I2MTC)*, 2023. DOI: 10.1109/I2MTC53148.2023.10175924

discussed. Electrostatic simulations of probe circuit coupling capacitances are described in Section IV. RF voltage measurements on test structures are presented in Section V. Section VI concludes the paper.

II. System description

Fig. 1 shows the working principle of the RF voltage sensing system [12]. The RF voltage U on a test point on the device under test (DUT) is measured. To this end, a cantilever probe with a sharp tip is brought in proximity to the surface and couples to the test point with a capacitance C. The probe is mounted to an open-ended transmission line in order to transmit the detected signal to a vector network analyser (VNA). The resulting voltage measured by the VNA therefore equals [13]

$$U_m = U \cdot \frac{j\omega Z_0 C}{1 + j\omega Z_0 C} \approx U \cdot j\omega Z_0 C\,, \tag{1}$$

where ω, and $Z_0 = 50\,\Omega$ denote the circular frequency and the characteristic impedance, respectively. The assumption in (1) requires $\omega Z_0 C \ll 1$, which is valid for the used frequencies ($\omega \leq 2\pi \cdot 13\,\mathrm{GHz}$) and tip circuit capacitances ($C < 1\,\mathrm{fF}$) in this work.

As shown in Fig. 1, in miniaturized microwave devices the probe in general shows not only a capacitance to the test point at voltage U, but also capacitances (C_{c1} and C_{c2}) to adjacent test points at different voltages (U_{c1} and U_{c2}). To ensure that the gradient of the local capacitance C dominates the overall coupling capacitances to the circuit, the tip apex size must be similar to or smaller than the size and separations of the test points. Additionally, an accurate knowledge of the tip-surface distance is required for achieving a well-defined tip-circuit capacitance, as well as to enable the correction of cross-talk induced errors by a model-based measurement procedure.

A. Probe description and positioning

A metal cantilever (25Pt300C, Rocky Mountain Nanotechnology, USA) is used as probe. The cantilever has a length of 300 μm and is commonly used in Scanning Microwave Microscopy [14], [15]. The tip at the end of the cantilever is 80 μm long and has a sharp apex ($< 20\,\mathrm{nm}$ radius). The probe is mounted and electrically contacted to the end of a grounded coplanar waveguide (GCPW), which is implemented on a low-loss material (Rogers 4003C) and can be connected by an SMA-connector. The capability of transmitting RF signals with frequencies of up to 13 GHz from the tip to the VNA has been demonstrated [12].

A high precision positioning system is used to move the GCPW and thus the probe relative to the DUT. The positioning system is integrated in a custom-built measurement head and consists of a two-axis piezo stage (NPXY100-100, nPoint, USA) for horizontal probe movement, and a piezoelectric actuator with integrated strain gauges (PC4WMC2, Thorlabs, USA) for vertical probe movement. As shown in Fig. 1, the deflection of the cantilever is measured by a laser-based deflection sensor. Together with the position measurement

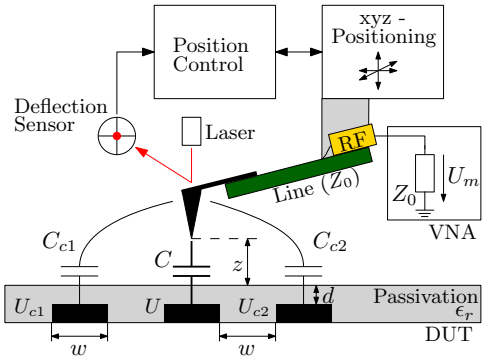

Fig. 1: Block diagram of the implemented RF voltage sensing system and illustration of the device under test (DUT).

of the piezoelectric actuator, this enables a precise detection of the vertical position where mechanical tip-surface contact occurs.

B. Device under test

Interdigital capacitance structures are used to evaluate the spatial resolution of the RF sensing system. As shown in the cross-section in Fig. 1, the width of the individual electrodes is identical to the gap between the electrodes. Multiple structures with sizes w ranging from 2 μm to 5 μm are implemented on a test chip. The test chip is covered with a passivation layer with a thickness of $d = 1.5\,\mu\mathrm{m}$ and a permittivity of $\epsilon_r = 4$. One side of the capacitance structure is connected to a transmission line which is contacted by a ground-signal-ground RF probe, the other side is connected to ground. The individual electrodes are therefore subsequently connected to the applied RF voltage and to ground.

III. Model-based RF voltage sensing

The horizontal placement of the probe over the DUT strongly affects the vertical distance dependence of the capacitance between the tip and different test points on the circuit. By performing a continuous measurement of the RF voltage vs. distance, cross-talk from adjacent circuit parts can therefore be reduced by employing a suitable model of the tip-circuit capacitance [12].

The capacitance between a cone shaped tip and an electrode beneath a thin passivation layer can in general be modelled as superposition of a short-range capacitance with a non-linear distance dependence, and a long-range capacitance with a linear distance dependence [16]. For the RF sensing configuration in Fig. 1, the capacitance C between the tip and the electrode closest to the tip can therefore be defined as

$$C(z) = C_{nl}(z) + C_{lin}(z)\,. \tag{2}$$

The short-range capacitance $C_{nl}(z)$ is modelled by [16]

$$C_{nl}(z) = 2\pi\epsilon_0 R \cdot \ln\left(1 + \frac{R}{z + \frac{d}{\epsilon_r}}\right)\,, \tag{3}$$

Pre-print version of the article: Mathias Poik, Thomas Hackl, Stefano Di Martino, Martin Schober, Jin Dang and Georg Schitter, "Analysis of Cross-Talk Induced Measurement Errors in Model-Based RF Voltage Sensing ", *2023 IEEE International Instrumentation and Measurement Technology Conference (I2MTC)*, 2023. DOI: 10.1109/I2MTC53148.2023.10175924

where d and ϵ_r denote the thickness and the relative permittivity of the passivation layer, R is an effective tip apex radius and ϵ_0 denotes the free space permittivity. The long-range capacitance $C_{lin}(z)$ has a purely linear distance dependence. The parasitic coupling capacitances C_{c1} and C_{c2} can be similarly defined as

$$C_{ci}(z) = \underbrace{C_{ci,nl}(z)}_{\approx 0} + C_{ci,lin}(z)\,, \quad i = 1, 2\,. \tag{4}$$

However, according to the simplified model, the short-range capacitance is close to zero due to the larger distance between tip and the adjacent electrodes. As a result, using (1), the total voltage measured by the VNA depending on the tip-surface distance can be written as

$$U_m(z) \propto C_{nl}(z)U + \underbrace{\left[C_{lin}(z)U + \sum_{i=1}^{2} C_{ci,lin}(z)U_{ci}\right]}_{U_{lin}(z)}\,. \tag{5}$$

The measured voltage is therefore given by a superposition of two terms. The term with non-linear distance dependence is defined only by the local voltage U, while the term with linear distance dependence is generated by the sum of all parasitic capacitance contributions between the tip and other parts of the DUT.

If a voltage measurement at multiple tip-surface distances is available, cross-talk can be avoided by identifying the non-linear distance dependence. The voltage (5) can be rewritten as

$$U_m(z) \propto C_{nl}(z)U_n + U_{lin}(z)\,, \tag{6}$$

where the weighting factor U_n corresponds to the local voltage. The procedure for measuring the local RF voltage at a given test point therefore consists of recording $U_m(z)$ for a suitable range of distances, followed by a fit of the model (6) in order to identify U_n.

A. Measurement procedure

To demonstrate the procedure, a measurement is performed with the tip placed over a 5 μm wide electrode as shown in Fig. 1. An RF voltage with an amplitude $U = 1\,\mathrm{V}$ at a frequency of 13 GHz is applied to the electrode. The voltage U_m is recorded while the tip approaches the surface by applying a ramp signal to the vertical piezoelectric actuator. Fig. 2 shows $U_m(z)$ depending on the tip-surface distance. The dashed line shows the model which is fitted to the measured data by means of a least squares fit. The effective tip radius R describes the geometry of the tip. Although the manufacturer specifies a physical tip apex radius of 20 nm, it is known that the soft metal tip of the used cantilever probes can easily deform or bend, thus increasing the effective radius up to the µm range [17]. In this work a radius of $R = 0.96\,\mu\mathrm{m}$ is used since it provides the best fit to the measurement data. The influence of the tip radius is analyzed in more detail in Section IV-B. The measurement distance in Fig. 2 is selected as small as possible to achieve a minimum measurement duration, while it has to be large enough to ensure that the linear distance dependence can still be identified.

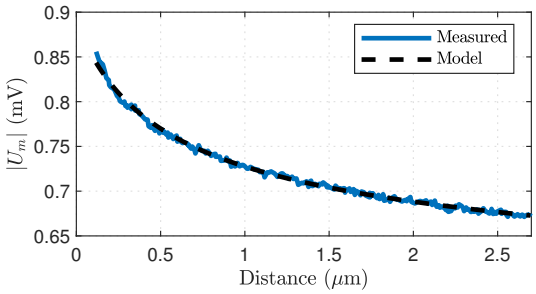

Fig. 2: Procedure for model-based RF voltage sensing. The magnitude of U_m is recorded depending on the tip-surface distance and (6) is fitted to the measurement data.

B. Limitations

The described model-based measurement method requires that parasitic coupling capacitances to adjacent electrodes on the circuit have a predominantly linear tip-surface distance dependence. Specifically, the term $C_{ci,nl}$ in (4) has to be small with respect to the term C_{nl} in (2). It is clear that this assumption can only be valid if the distance of adjacent electrodes to the tip is sufficiently large. For instance, an underlying assumption for the validity of the capacitance model (2)-(3) is that the electrode size is large with respect to the tip radius [16]. This assumption no longer holds as the width and the gap between electrodes is reduced towards the range of single μm. In the following, the limitations of the model-based measurement method are analysed by electrostatic simulations of the coupling capacitances between the tip and test points on the circuit.

IV. Analysis of Tip-Circuit Capacitance

A. Electrostatic simulation

Electrostatic simulations of the tip-circuit capacitances are carried out in Comsol (Comsol Multiphysics GmbH, Germany). The total simulation volume is $50 \times 50 \times 50\,\mu\mathrm{m}$. The upper half is air and contains the cone shaped tip with a height of $25\,\mu\mathrm{m}$ and a spherical apex with a radius of $R = 0.96\,\mu\mathrm{m}$. The bottom half is modelled as dielectric with relative permittivity $\epsilon_r = 4$ and includes the electrodes with a width and separation w and a length of $25\,\mu\mathrm{m}$ (perpendicular to the cross-section in Fig. 1). The coupling capacitances between the tip and the electrodes are simulated for distances of $0.1\,\mu\mathrm{m}$ to $2.7\,\mu\mathrm{m}$ corresponding to the measurement parameters. For the simulations the tip is always located in the center (horizontally) of the middle electrode on the DUT. The actual DUT contains additional structures, such as the connection of the electrodes to contact pads for applying RF signals and to ground. However, since only the relative change of the capacitances for a small vertical probe movement is considered, it is expected that structures at a larger distance

Pre-print version of the article: Mathias Poik, Thomas Hackl, Stefano Di Martino, Martin Schober, Jin Dang and Georg Schitter, "Analysis of Cross-Talk Induced Measurement Errors in Model-Based RF Voltage Sensing ", *2023 IEEE International Instrumentation and Measurement Technology Conference (I2MTC)*, 2023. DOI: 10.1109/I2MTC53148.2023.10175924

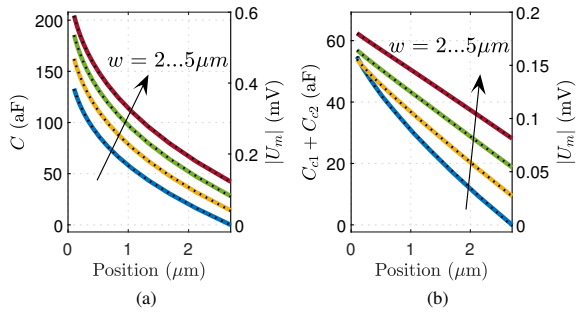

Fig. 3: Electrostatic simulation of (a) capacitance C between tip and electrode closest to the tip and (b) capacitance $C_{c1} + C_{c2}$ to adjacent electrodes on the DUT. The arrows indicate increasing sizes (2, 3, 4 and 5 μm). The axes on the right side denote the calculated voltage U_m according to (1).

are negligible for the analysis of the model validity. Based on the same assumption it is expected that the influence of the cantilever, as well as of upper parts of the tip cone, are negligible.

Fig. 3a shows the results of the simulated capacitances C between the tip and the electrode directly below the tip. Fig. 3b shows the simulated coupling capacitances $C_{c1}+C_{c2}$ between the tip and the adjacent electrodes in Fig. 1. The value at $z = 2.7\,\mu$m is subtracted and the curves are offset by a constant value for better visibility. The values depicted on the right axes show the expected voltage which would be measured by the VNA for the simulated capacitance values according to (1). This assumes that for the results in Fig. 3a the tip is placed over an electrode connected to an RF voltage, with the adjacent electrodes connected to ground. Vice versa, for the results in Fig. 3b the tip is assumed to be placed over a grounded electrode with the adjacent electrodes connected to an RF voltage. The dashed lines show the fitted model according to (6) for each measurement.

The simulated capacitances C closely fit the simplified model, showing that it can be modelled as superposition of a long-range linear term and a short-range non-linear term. The extent of the non-linear increase is similar for all simulated structure sizes. The results in Fig. 3b show a close to linear distance dependence. The slope reduces with increasing structure size, which can be explained by the increasing gap and thus larger distance between the structures. For the structure size $w = 2\,\mu$m, the simulation in Fig. 3b appears to deviate from the expected linear dependence for small distances, indicating a limited validity of the model for small structures.

B. Validity of model-based measurement method

For a quantitative evaluation of the validity of the simplified model presented in Section III, the parameter U_n is identified for all curves in Fig. 3 by applying a least squares fit. Fig. 4a shows the resulting identified parameters. The dotted line shows the results for the simulations in Fig. 3b. It can be

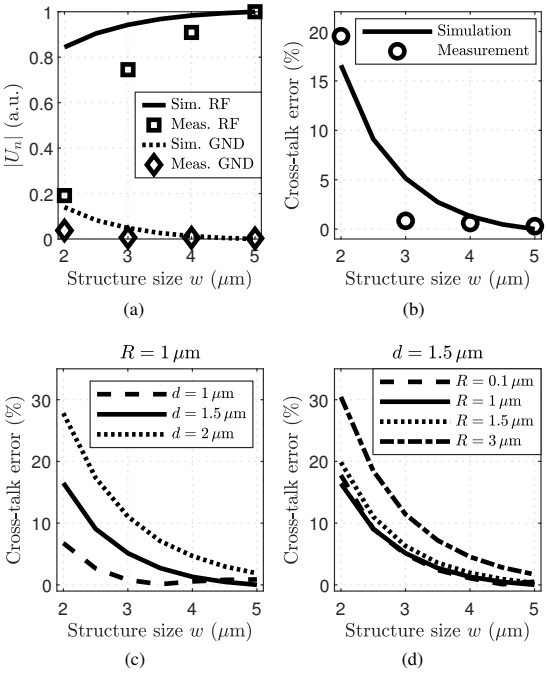

Fig. 4: (a) Simulation and measurement of non-linear contributions in U_m for different tip positions (at RF electrode / at grounded electrode). (b) Cross-talk induced error depending on structure size. (c) Influence of passivation thickness and (d) influence of tip radius on cross-talk induced error.

seen that the identified U_n is small for larger structure size as expected from the close to linear distance dependence. For smaller structure sizes U_n deviates from zero indicating a limited validity of the model due to the now small distance of the adjacent electrodes from the tip. The continuous line corresponds to the simulations in Fig. 3a and shows a decrease of U_n with decreasing structure size. This can be explained by the fact that the used non-linear model in (3) requires that the electrode size is significantly larger than the tip apex radius, which is no longer valid in this case.

Fig. 4b shows the ratio between the identified parameters for the simulations at a grounded electrode ($C_{c1}+C_{c2}$) and the electrode connected to an RF voltage (C). Since the model-based measurement method requires that $C_{ci,nl}$ in (4) is small with respect to C_{nl} in (2), this ratio corresponds to the cross-talk induced error of the method. The results show that for a tip radius of $R = 0.96\,\mu$m and a passivation thickness of $d = 1.5\,\mu$m cross-talk increases significantly for structure sizes smaller than about $3\,\mu$m.

Fig. 4c shows the cross-talk induced error depending on the thickness of the passivation layer. It can be seen that the passivation thickness has a significant impact on the achievable spatial resolution of the model-based measurement method. Comparing the simulations for a small value of 5 % shows that

Pre-print version of the article: Mathias Poik, Thomas Hackl, Stefano Di Martino, Martin Schober, Jin Dang and Georg Schitter, "Analysis of Cross-Talk Induced Measurement Errors in Model-Based RF Voltage Sensing ", *2023 IEEE International Instrumentation and Measurement Technology Conference (I2MTC)*, 2023. DOI: 10.1109/I2MTC53148.2023.10175924

the error scales roughly linear with d and limits the minimum structure size to about twice the thickness of the passivation layer. Fig. 4d shows the influence of the tip radius on the error for a constant passivation thickness. The error remains roughly constant for a tip radius up to $1.5\,\mu$m, which shows that for the used probe the error is mainly defined by the passivation layer thickness.

The simulations of the tip-circuit coupling capacitances indicate that model-based RF sensing enables the correction of cross-talk induced errors for local voltage measurements on structures with a minimum size of twice the passivation layer thickness.

V. Measurement Results

To verify the electrostatic simulation results RF voltage vs. distance curves are carried out on two different locations on the DUT. First the tip is placed over electrodes connected to an RF voltage with an amplitude $U = 1\,\mathrm{V}$, with the adjacent electrodes connected to ground ($U_{c1} = U_{c2} = 0$). Since the coupling capacitance C_{c1} and C_{c2} therefore have no impact on the measured voltage U_m, the result is expected to be proportional to the capacitance C according to (1). In the second measurement the tip is placed over a grounded electrode ($U = 0$) with the adjacent electrodes connected to $U_{c1} = U_{c2} = 1\,\mathrm{V}$. Therefore C has no impact and the resulting measured voltage U_m should be proportional to the coupling capacitances $C_{c1} + C_{c2}$. The frequency of the applied signals is 13 GHz for all measurements.

Fig. 5a and Fig. 5b show the resulting voltages U_m for the two measurement positions depending on the tip-surface distance. The dashed line shows the fitted model according to (6). The measurement results confirm the close agreement of the tip-circuit capacitance with the used model. The measured voltage U_m at the RF electrode (Fig. 5a) shows a non-linear increase for all structure sizes as the distance approaches the tip radius. The absolute values of the local increase are similar to the simulated result, which verifies that the simulated capacitance values in the range of 50 to 100 aF are close to the actual local tip-circuit capacitances. The voltage at the grounded electrode (Fig. 5b) shows a close to linear distance dependence, with a reducing slope for increasing structure sizes. It is noted that the scaling of the axes in the measurement is reduced by a factor of 2 with respect to the simulation. It appears that the actual long-range linear contribution is significantly smaller than simulated, which may be due to the simplified 3D model used in the simulation. However, since the model-based method merely requires that the long-range contribution has a linear distance dependence, the actual slope is not relevant for the validity of the method.

The cross-talk induced measurement error is analysed by comparing the identified parameter U_n in all fitted curves. The resulting parameters for different structure sizes are depicted in Fig. 4a together with the simulation results. For the measurements on the RF electrode in Fig. 5a the identified U_n reduces with decreasing structure size. This is consistent with the simulation, although it appears that the structure

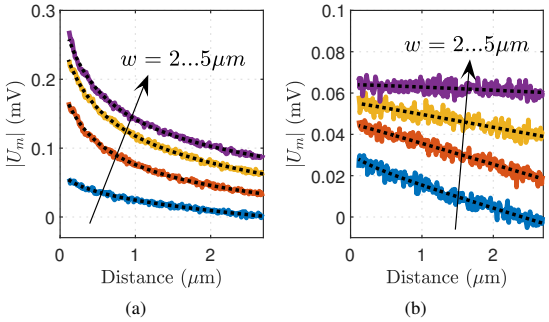

Fig. 5: Measured voltage U_m depending on the distance. The tip is placed over (a) an electrode connected to an RF voltage $U = 1\,\mathrm{V_{pk}}$, (b) a grounded electrode. The arrows indicate increasing sizes (2, 3, 4 and 5 μm).

size actually has are larger influence on the non-linear tip circuit capacitance than expected from the simulation results. Similarly, the identified U_n for the measurements in the grounded electrode in Fig. 5a increases for reducing structure sizes, albeit less than in the simulation, indicating that the non-linear capacitance contribution of adjacent electrodes is smaller than expected. Fig. 4b shows the computed ratio of the identified parameters. It can be seen that the cross-talk induced error is small for structure sizes $\geq 3\,\mu$m, while it increases significantly for the measurements on the structure with $w = 2\,\mu$m, which is consistent with the simulated result.

To demonstrate the capability of the RF sensing system to measure voltages at different locations on the surface, measurements on a line along the cross-section of the DUT are performed. As in the previous analysis, the interdigital capacitance structures are supplied by RF voltages with an amplitude of 1 V and a frequency of 13 GHz. At each location, an RF voltage vs. distance curve is recorded and the parameter U_n is identified. Fig. 6 shows the resulting RF voltages for different structure sizes from $2\,\mu$m to $5\,\mu$m as denoted in the figure caption. For an electrode size $\geq 3\,\mu$m the voltage at the grounded electrodes can be correctly identified as zero, while for the $2\,\mu$m structures cross-talk induced by the adjacent electrodes leads to a measurement error.

For simplicity, only structures with identical widths and gaps are considered for the analysis in this work. However, it is noted that in Fig. 6c-d the gaps to the two outermost electrodes deviate from the mentioned sizes. For instance, in Fig. 6d this gap is $3.2\,\mu$m and the voltage at the grounded electrode is close to the expected value of zero. This shows, that the correction of cross-talk is also possible for RF voltage measurements at smaller (than $3\,\mu$m) test points, if the gaps are sufficiently large.

In summary, it has been shown that cross-talk induced measurement errors limit the achievable spatial resolution of model-based RF sensing on passivated devices to two times the passivation layer thickness.

Pre-print version of the article: Mathias Poik, Thomas Hackl, Stefano Di Martino, Martin Schober, Jin Dang and Georg Schitter, "Analysis of Cross-Talk Induced Measurement Errors in Model-Based RF Voltage Sensing ", *2023 IEEE International Instrumentation and Measurement Technology Conference (I2MTC)*, 2023. DOI: 10.1109/I2MTC53148.2023.10175924

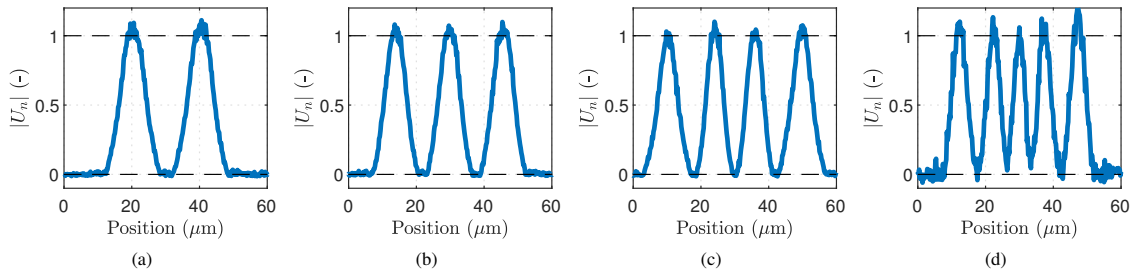

Fig. 6: Measurement of RF voltages in interdigital capacitance structures with electrode sizes of (a) 5 μm, (b) 4 μm, (c) 3 μm and (d) 2 μm. The results are normalized to the measured values at the respective electrodes connected to the RF signal.

VI. Conclusion

Contactless RF measurements by passive voltage probes are limited by cross-talk to adjacent circuit parts. The analysis presented in this paper shows that cross-talk can be reduced by recording voltages at multiple tip-surface distances and identifying parameters of a simplified capacitance model, thus enabling contactless measurements with µm spatial resolution. The method is based on the assumption, that the distance dependence of tip-circuit capacitances can be modelled by the superposition of a short-range non-linear term and a long-range linear term. To analyse the validity of this assumption, coupling capacitances between a probe tip and test structures with different sizes are analysed by electrostatic simulations. The simulation shows that a passivation layer on the device under test limits the minimum structure size for which the correction of cross-talk is possible to about two times the layer thickness. The simulation results are verified by RF measurements at a frequency of 13 GHz on interdigital capacitance structures with sizes down to 2 μm.

Acknowledgment

The authors would like to thank Bernhard Berger, Thomas Thurner and Sebastian Sattler for their support. The financial support by the Austrian Science Fund FWF (Project Nr. P 31238-N28) and the FFG Production of the Future programme (Project Nr. 883916) of the Austrian BMK is gratefully acknowledged.

References

[1] A. Joseph, A. Botula, J. Slinkman, R. Wolf, R. Phelps, M. Abou-Khalil, J. Ellis-Monaghan, S. Moss, and M. Jaffe, "Power handling capability of an SOI RF switch," in *Digest of Papers - IEEE Radio Frequency Integrated Circuits Symposium*, 2013, pp. 385–388.

[2] D. Denis, C. M. Snowden, and I. C. Hunter, "Coupled Electrothermal, Electromagnetic, and Physical Modeling of Microwave Power FETs," *IEEE Transactions on Microwave Theory and Techniques*, vol. 54, no. 6, pp. 2465–2470, 2006.

[3] M. Rigato, C. Fleury, B. Schwarz, M. Mergens, S. Bychikhin, W. Simburger, and D. Pogany, "Analysis of ESD Behavior of Stacked nMOSFET RF Switches in Bulk Technology," *IEEE Transactions on Electron Devices*, vol. 65, no. 3, pp. 829–837, 2018.

[4] V. Solomko, O. Oezdamar, R. Weigel, and A. Hagelauer, "Model of Substrate Capacitance of MOSFET RF Switch Inspired by Inverted Microstrip Line," in *ESSDERC 2021 - IEEE 51st European Solid-State Device Research Conference (ESSDERC)*, Sep. 2021, pp. 207–210.

[5] D. Uchida, T. Nagai, Y. Oshima, and S. Wakana, "Novel high-spatial resolution probe for electric near-field measurement," in *2011 IEEE Radio and Wireless Week, RWW 2011 - 2011 IEEE Radio and Wireless Symposium, RWS 2011*. IEEE, 2011, pp. 299–302.

[6] R. Hou, M. Spirito, R. Heeres, F. Van Rijs, and L. C. De Vreede, "Non-intrusive near-field characterization of distributed effects in large-periphery LDMOS RF power transistors," *2015 IEEE MTT-S International Microwave Symposium, IMS 2015*, pp. 1–3, 2015.

[7] N. Dehghan and S. C. Cripps, "A novel in-situ calibration technique for a high resolution E-Field probe," in *2015 IEEE MTT-S International Microwave Symposium*. IEEE, 2015.

[8] R. Hou, M. Lorenzini, M. Spirito, T. Roedle, F. van Rijs, and L. C. N. de Vreede, "Nonintrusive Near-Field Characterization of Spatially Distributed Effects in Large-Periphery High-Power GaN HEMTs," *IEEE Transactions on Microwave Theory and Techniques*, vol. 64, no. 11, pp. 4048–4062, 2016.

[9] N. Dehghan, "High Resolution Electric Field Probes with Applications in High Efficiency RF Power Amplifier Design," Dissertation, Cardiff University, 2014.

[10] D. Baudry, A. Louis, and B. Mazari, "Characterization of the Open-Ended Coaxial Probe Used for Near-Field Measurements in Emc Applications," *Progress In Electromagnetics Research*, vol. 60, pp. 311–333, 2006.

[11] R. Kantor and I. V. Shvets, "Measurement of electric-field intensities using scanning near-field microwave microscopy," *IEEE Transactions on Microwave Theory and Techniques*, vol. 51, no. 11, pp. 2228–2234, 2003.

[12] M. Poik, T. Hackl, S. Di Martino, M. Schober, J. Dang, and G. Schitter, "Model-Based RF Sensing for Contactless High Resolution Voltage Measurements," **Submitted** to *IEEE Transactions on Instrumentation and Measurement*.

[13] W. Fang, H. Qiu, C. Luo, L. Wang, W. Shao, E. Shao, S. Li, and Y. En, "Noncontact RF Voltage Sensing of a Printed Trace via a Capacitive-Coupled Probe," *IEEE Sensors Journal*, vol. 18, no. 21, pp. 8873–8882, 2018.

[14] G. Gramse, M. Kasper, L. Fumagalli, G. Gomila, P. Hinterdorfer, and F. Kienberger, "Calibrated complex impedance and permittivity measurements with scanning microwave microscopy," *Nanotechnology*, vol. 25, no. 14, 2014.

[15] P. Polovodov, D. Théron, C. Lenoir, D. Deresmes, S. Eliet, C. Boyaval, G. Dambrine, and K. Haddadi, "Near-Field Scanning Millimeter-Wave Microscope Operating Inside a Scanning Electron Microscope: Towards Quantitative Electrical Nanocharacterization," *Applied Sciences*, vol. 11, no. 6, p. 2788, Jan. 2021.

[16] L. Fumagalli, G. Ferrari, M. Sampietro, I. Casuso, E. Martinez, J. Samitier, and G. Gomila, "Nanoscale capacitance imaging with attofarad resolution using ac current sensing atomic force microscopy," *Nanotechnology*, vol. 17, no. 18, pp. 4581–4587, 2006.

[17] I. Humer, C. Eckhardt, H. P. Huber, F. Kienberger, and J. Smoliner, "Tip geometry effects in dopant profiling by scanning microwave microscopy," *Journal of Applied Physics*, vol. 111, no. 4, p. 044314, Feb. 2012.

Pre-print version of the article: Mathias Poik, Thomas Hackl, Stefano Di Martino, Martin Schober, Jin Dang and Georg Schitter, "Analysis of Cross-Talk Induced Measurement Errors in Model-Based RF Voltage Sensing ", *2023 IEEE International Instrumentation and Measurement Technology Conference (I2MTC)*, 2023. DOI: 10.1109/I2MTC53148.2023.10175924